ACS Chemical Neuroscience

pubs.acs.org/chemneuro

Research Article

Photoactivatable Dopamine and Sulpiride to Explore the Function of Dopaminergic Neurons and Circuits

Naeem Asad, Duncan E. McLain, Alec F. Condon, Sangram Gore, Shahienaz E. Hampton, Sauparnika Vijay, John T. Williams,* and Timothy M. Dore*

Cite This: *ACS Chem. Neurosci.* 2020, 11, 939–951

Read Online

ACCESS | Metrics & More | Article Recommendations | Supporting Information

ABSTRACT: Kinetic analysis of dopamine receptor activation and inactivation and the study of dopamine-dependent signaling requires precise simulation of the presynaptic release of the neurotransmitter dopamine and tight temporal control over the release of dopamine receptor antagonists. The 8-cyano-7-hydroxyquinolinyl (CyHQ) photoremovable protecting group was conjugated to dopamine and the dopamine receptor antagonist sulpiride to generate "caged" versions of these neuromodulators (CyHQ-*O*-DA and CyHQ-sulpiride, respectively) that could release their payloads with 365 or 405 nm light or through 2-photon excitation (2PE) at 740 nm. These compounds are stable under physiological conditions in the dark, yet photolyze rapidly and cleanly to yield dopamine or sulpiride and the caging remnant CyHQ−OH. CyHQ-*O*-DA mediated the light activation of dopamine-1 (D1) receptors on the breast cancer cell line MDA-MB-231 in culture. In mouse brain slice from the substantia nigra pars compacta, localized flash photolysis of CyHQ-*O*-DA accurately mimicked the natural presynaptic release of dopamine and activation of dopamine-2 (D2) receptors, causing a robust, concentration-dependent, and repeatable G protein-coupled inwardly rectifying potassium channel-mediated outward current in whole-cell voltage clamp recordings that was amplified by cocaine and blocked by sulpiride. Photolysis of CyHQ-sulpiride rapidly blocked synaptic activity, enabling measurement of the unbinding rates of dopamine and quinpirole, a D2 receptor agonist. These tools will enable more detailed study of dopamine receptors, their interactions with other GPCRs, and the physiology of dopamine signaling in the brain.

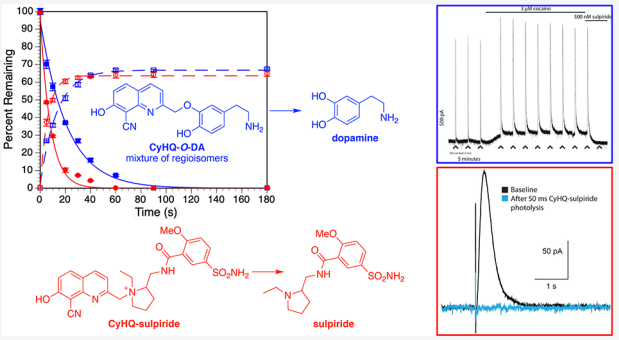

KEYWORDS: *photoremovable protecting groups, caged compounds, photoactivation, neuromodulators, dopamine, sulpiride*

INTRODUCTION

Dopamine is the primary agonist of the dopamine receptor,[1,2] of which five subtypes exist: D1−D5. Abnormal dopaminergic function is implicated in diseases and disorders like Parkinson's disease,[3] Alzheimer's disease,[4] schizophrenia,[5] addiction,[6] bipolar disorder,[7] and attention-deficit hyperactivity disorder (ADHD).[8] Dopamine signaling also underlies the regulation of movement and plays an important role in reward driven learning.[9,10] A complete understanding of the mechanisms that underlie these processes has been the source of considerable effort.[11] To this point, there are few studies that have been able to determine how dopamine receptors signal with precise spatial and temporally relevant application of dopamine.[12−14] Synaptic release from vesicular stores results in a high local concentration of dopamine in the extracellular space that is removed through the reuptake by the plasma membrane-associated dopamine transporter.[15−18] To understand dopamine-dependent signaling, it is necessary to apply exogenous dopamine with similar precision to mimic the natural release of the neurotransmitter. Studies have been hampered in this way because diffusion barriers in the brain pose a significant limitation on the speed at which dopamine can be applied. Thus, the kinetic analysis of receptor activation and inactivation has not been adequately addressed. This problem can be overcome with the use of "caged" agonists and antagonists that can be photoactivated with submicrosecond precision.[19] The term "caged compound" used here means an agonist or antagonist covalently bound to a photoremovable protecting group (PPG), inactivating the agonist or antagonist by greatly reducing its affinity for its target receptor. Light cleaves the bond to release the active form of the agonist or antagonist.[20] PPG-effector conjugates or caged compounds offer the ability to rapidly release dopamine or an antagonist, such as the D2 and D3 receptor-selective inhibitor

Received: December 19, 2019
Accepted: February 20, 2020
Published: February 20, 2020

https://dx.doi.org/10.1021/acschemneuro.9b00675
ACS Chem. Neurosci. 2020, 11, 939–951

sulpiride,[21−23] and enable kinetic analyses that have not been possible previously.

A number of caged dopamine compounds have been produced: CNB-,[24] NPEC-, RuBi-,[25] BBHCM-,[26] and CNV-caged[27] dopamine (Figure 1). Quantitative photochemical

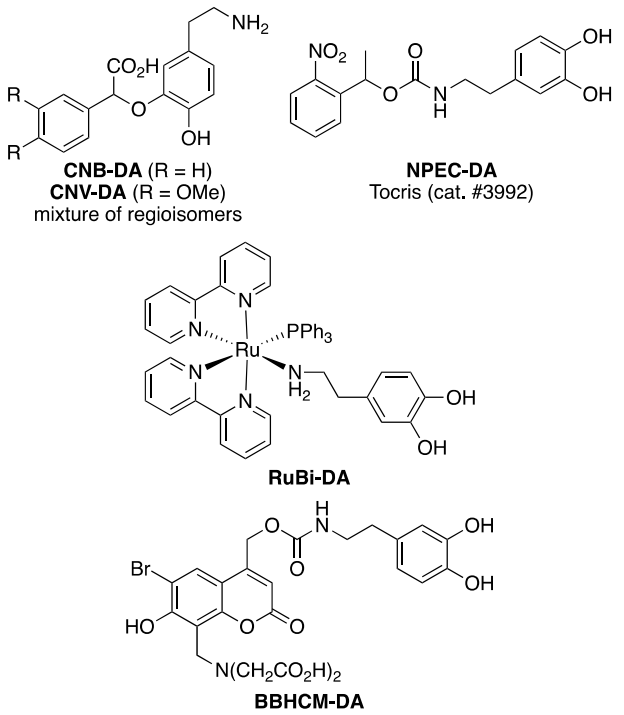

Figure 1. Photoactivatable dopamine derivatives.

property data are not reported for CNB-, CNV-, and NPEC-DA. The CNB group has a short maximum excitation wavelength (λ_{max} = 266 nm)[28] with little absorptivity at wavelengths >350 nm,[29] where light is less likely to cause damage. CNV-DA improved on this and can be excited at 365 nm.[27,30] For tight spatial resolution of dopamine release in cell culture, the release kinetics should be faster than rates of diffusion out of the focal volume of the light beam, i.e., time scales less than 1 ms.[31,32] The CNB and CNV groups depend on the decomposition of excited state intermediates that occur on time scales of 20−80 μs,[29,30,33,34] but the NPEC PPG releases on millisecond to second time scales.[35] NPEC- and BBHCM-dopamine are also slow to release dopamine because they contain carbamate linkages, which after photolytic cleavage of the C−O bond slowly decompose on millisecond to second time scales to reveal the amine.[36,37] Data on the stability toward spontaneous release of dopamine in the dark from CNB-, CNV-, NPEC-, and RuBi-DA are not reported, although the CNV-protected phenolic ether of capsaicin decomposed 1.7% in 24 h in pH 7.2 HEPES buffer.[38] In physiological buffer, BBHCM-dopamine decomposed 7% in 24 h.[26] Both of these hydrolysis rates should not significantly impact experiments of short duration. We have observed that repeated photolysis of RuBi-DA on brain slice did not give a consistent electrophysiological response over time (Figure S1). If tight 3-dimesional control over dopamine release through 2-photon excitation (2PE)[39−42] in tissue culture is desired, then the BBHCM and RuBi groups have much higher sensitivities to this mode of excitation than the CNB-, CNV-, and NPEC groups, which probably behave like related nitrobenzyl-based PPGs in being practically insensitive to 2PE.[20,40,43]

A photoactivatable form of sulpiride has not been reported previously, but 2-nitrobenzyl- and dimethoxynitrobenzyl-protected D2/D3 receptor antagonist, dechloroeticlopride, were recently reported.[44] Effective caged antagonists are more challenging to create than those of agonists because most antagonists are highly potent with IC_{50} values in the low nanomolar range. A small amount of spontaneous hydrolysis in the dark of the PPG-antagonist conjugate can cause a significant physiological effect. This challenge would need to be overcome for sulpiride, which is a potent antagonist of the human and rat D2 receptors with low nanomolar inhibitory constants (K_i = 9.4 and 6.9 nM, respectively).[22]

The present study describes the design and synthesis of caged dopamine derivatives and sulpiride using the 8-cyano-7-hydroxyquinolinyl (CyHQ) PPG.[45−48] A single photoactivatable dopamine, CyHQ-*O*-DA, emerged from among those prepared as having the most desirable physical and photochemical properties for in vivo use. CyHQ-*O*-DA and CyHQ-sulpiride are stable in physiological buffer and have rapid release kinetics and reasonable 2-photon uncaging action cross sections. CyHQ-*O*-DA photolyzed in cell culture and brain slices, where repeated applications of light rapidly activated D2 receptors in the substantia nigra resulted in reproducible outward currents. Likewise, photolysis of the CyHQ-protected sulpiride blocked D2 receptors, resulting in the rapid decline of the outward current induced by exogenously and synaptically applied dopamine.

RESULTS AND DISCUSSION

Synthesis. We prepared four different CyHQ-protected dopamine analogs, CyHQ-*O*-DA, $(CyHQ)_2$-*O*,*O*-DA, CyHQ-*N*-DA, and $(CyHQ)_2$-*N*,*O*-DA (Scheme 1). CyHQ-*O*-DA and CyHQ-*N*-DA were designed for rapid, clean photolysis reactions, although the initially formed carbamate from CyHQ-*N*-DA would be slow to release dopamine. $(CyHQ)_2$-*O*,*O*-DA and $(CyHQ)_2$-*N*,*O*-DA were designed to take advantage of chemical 2-photon uncaging,[49] which uses two PPGs bound to dopamine to severely diminish its ability to bind to dopamine receptors and provide robust hydrolytic stability. CyHQ-sulpiride (Scheme 2) was based on the ability of CyHQ to release tertiary amines.[47]

The synthesis of CyHQ-*O*-DA commenced with preparation of Boc-protected dopamine by an established procedure,[50] followed by reacting with MOM-CyHQ-OMs (prepared by literature procedures,[47] Scheme S1) and cesium carbonate in acetone to provide MOM-CyHQ-*O*-DA-Boc in 65% yield (Scheme 1). Treatment of MOM-CyHQ-*O*-DA-Boc with trifluoroacetic acid (TFA) in dichloromethane provided CyHQ-*O*-DA as a 10:7 mixture of regioisomeric ethers in 85% yield. $(CyHQ)_2$-*O*,*O*-DA was prepared by a similar strategy, but employing two equivalents of MOM-CyHQ-OMs. The resulting MOM-$(CyHQ)_2$-*O*,*O*-DA-Boc intermediate was deprotected with TMSCl in methanol, yielding $(CyHQ)_2$-*O*,*O*-DA. CyHQ-*N*-DA was synthesized by reacting MOM-CyHQ−OH (prepared by literature procedures,[47] Scheme S1) with 1,1′-carbonyldiimidazole (CDI) to generate an activated carbamate. The imidazole was displaced by dopamine, resulting in the formation of MOM-CyHQ-*N*-DA. Removal of the MOM ether was accomplished through treatment with TFA in dichloromethane to produce CyHQ-*N*-DA in 70% yield. $(CyHQ)_2$-*N*,*O*-DA was prepared by

https://dx.doi.org/10.1021/acschemneuro.9b00675
ACS Chem. Neurosci. 2020, 11, 939−951

Scheme 1. Synthesis of CyHQ-Protected Dopamine Derivatives

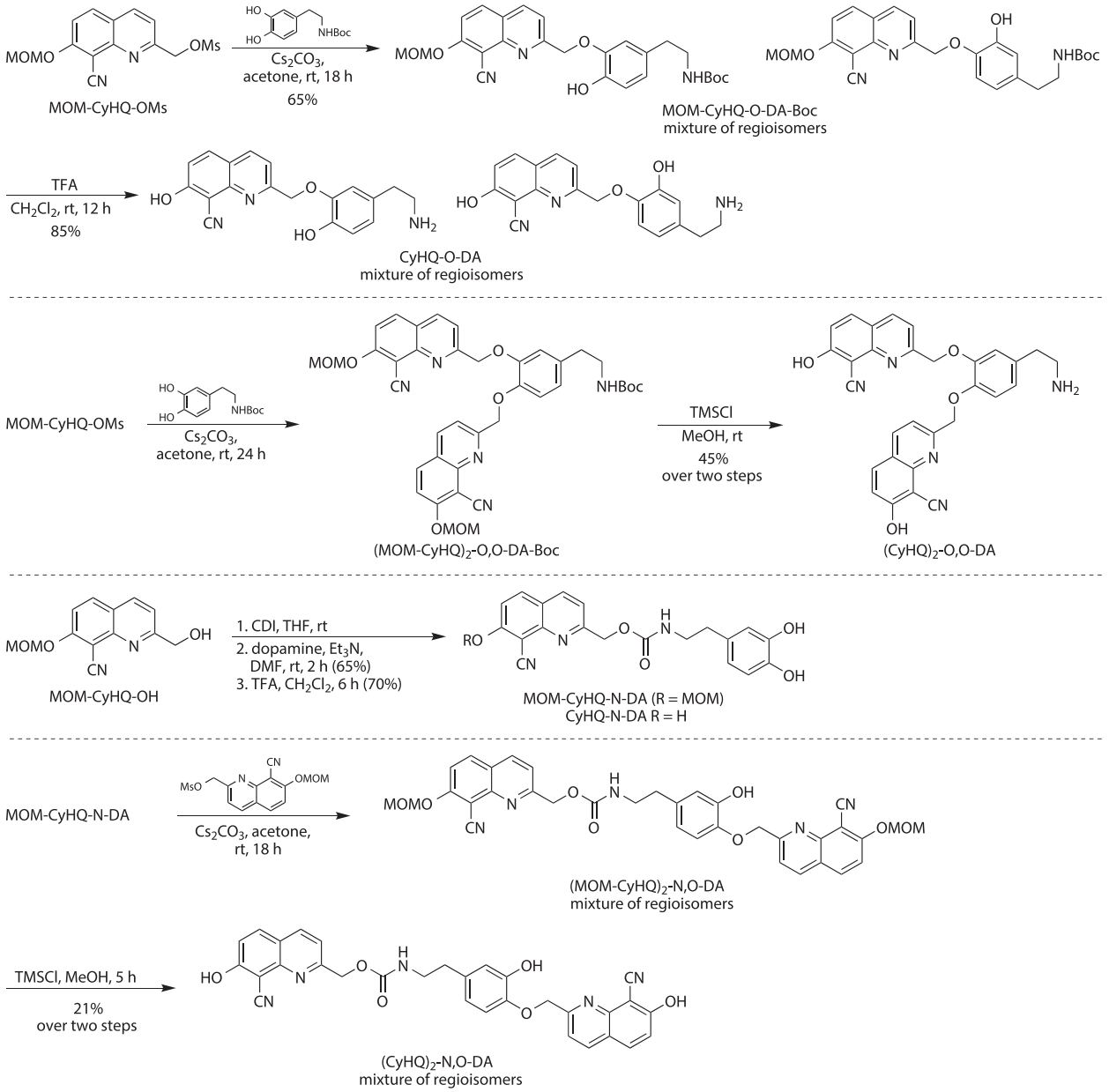

Scheme 2. Synthesis of CyHQ-Protected Sulpiride

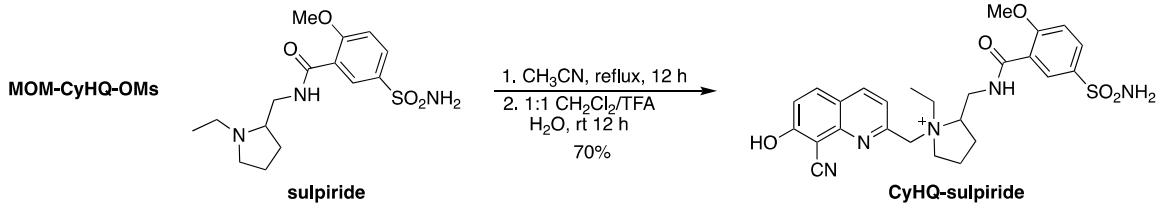

reacting MOM-(CyHQ)-*N*-DA with MOM-CyHQ-OMs using cesium carbonate in acetone as the base to generate MOM-$(CyHQ)_2$-*N*,*O*-DA. The deprotection was carried out with TMSCl in methanol to generate a 2:1 mixture of two regioisomers. CyHQ-sulpiride was synthesized by first reacting sulpiride and MOM-CyHQ-OMs in refluxing acetonitrile, followed by removal of the MOM group with TFA in dichloromethane (Scheme 2).

Photochemistry. The UV−vis spectra of each of the CyHQ-protected dopamine constructs in KMOPS buffer at pH 7.2 revealed reasonably strong absorptions (ε = 5300−8300 M^{-1} cm^{-1}) at 364−365 nm, including a tail that extended above 405 nm (Figure S2). A similar observation was made for CyHQ-sulpiride (Figure S2).

The photolysis reactions of the CyHQ-protected dopamine derivatives and sulpiride were assessed at 365 and 405 nm

https://dx.doi.org/10.1021/acschemneuro.9b00675
ACS Chem. Neurosci. 2020, 11, 939−951

Scheme 3. Photolysis Reactions of CyHQ-Protected Dopamine Derivatives and CyHQ-Protected Sulpiride

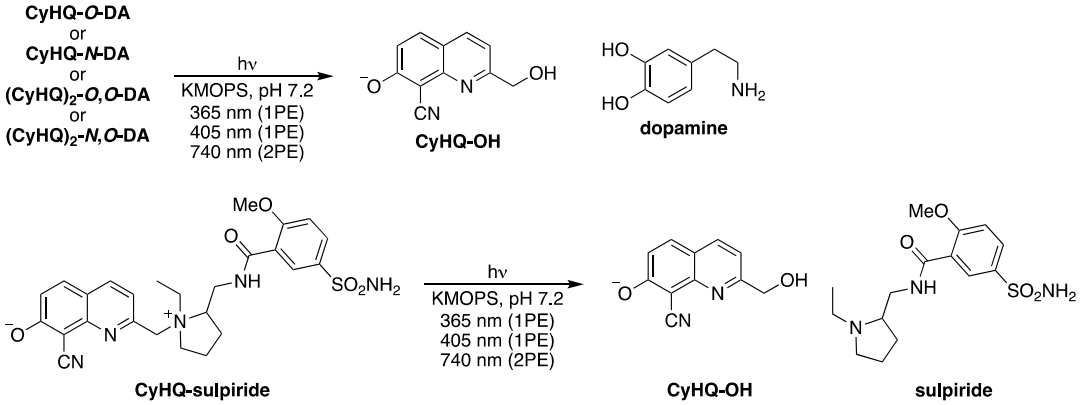

(1PE) under simulated physiological buffer conditions (pH 7.2 KMOPS buffer) using an LED light source at the respective wavelength (Scheme 3). The progress of each reaction was monitored by HPLC, detecting the disappearance of the CyHQ-protected dopamine or sulpiride and the appearance of free dopamine or sulpiride (Figure 2), and from these data the quantum yield (Φ_u) of the reaction and the chemical yield of dopamine or sulpiride were calculated (Table 1). The value of the 2-photon uncaging action cross-section (δ_u) was measured for CyHQ-*O*-DA, $(CyHQ)_2$-*O*,*O*-DA, and CyHQ-sulpiride (Figures S5 and S6); CyHQ-*N*-DA and $(CyHQ)_2$-*N*,*O*-DA did not photolyze through 2PE.

CyHQ-*O*-DA photolyzed with quantum yields of 0.19 and 0.20 at 365 and 405 nm, respectively, and released dopamine at 365 and 405 nm in 67 and 61% yield, respectively. CyHQ–OH and dopamine were the predominant products of the reaction; no significant amounts of other discrete photoproducts were detected. CyHQ-*O*-DA had a two-photon cross section of 0.24 GM. The value of Φ_u was slightly lower than that of other CyHQ-protected phenols, whereas the value of δ_u was similar to them.[46] $(CyHQ)_2$-*O*,*O*-DA displayed a photochemical quantum yield (0.19) and 2-photon uncaging action cross-section (δ_u = 0.12 GM), but yielded only 15−16% dopamine, perhaps owing to the fact that two independent photolysis reactions had to occur to release dopamine. (CyHQ)-*N*-DA was the most sensitive ($\varepsilon\cdot\Phi_u$) to photolysis through 1PE and gave a 60% yield of dopamine, but it was less stable in the dark than the ethers because the carbamate can hydrolyze in KMOPS, pH 7.2. In contrast to the other CyHQ-DA derivatives, $(CyHQ)_2$-*N*,*O*-DA exhibited low quantum and chemical yields of dopamine, possibly the result of a photophysical deactivation process from cross-talk between the chromophores.

CyHQ-sulpiride photolyzed with quantum yields of 0.19 and 0.22 at 365 and 405 nm, releasing sulpiride in 65 and 63%, respectively. Its sensitivity to 2PE at 740 nm, δ_u = 0.26 GM, was similar to that of other CyHQ-protected tertiary amines.[47]

The susceptibility of each CyHQ-protected dopamine derivative and sulpiride toward spontaneous hydrolysis in the dark was determined by monitoring the decomposition of a 100-μM solution of each in KMOPS buffer by HPLC. The concentration of CyHQ-*O*-DA and $(CyHQ)_2$-*O*,*O*-DA did not change over 100 h, that of CyHQ-*N*-DA and $(CyHQ)_2$-*N*,*O*-DA did not change over 24 h, and that of CyHQ-sulpiride did not change over 72 h, indicating that all of the compounds were sufficiently stable in the dark for biological experiments. All of the CyHQ-DA derivatives and CyHQ-sulpiride had adequate solubility for biological purposes; a 100-μM solution of each was easily prepared in KMOPS buffer.

CyHQ-*O*-DA portrayed the best photochemical and photophysical properties among all of the CyHQ-protected dopamine derivatives. Compared to previously reported PPG-dopamine conjugates, CyHQ-*O*-DA exhibited a higher quantum yield for 1PE than RuBi-[25] and BBHCM-DA[26] (Table 1). At their respective λ_{max} values, CyHQ-*O*-DA is more sensitive to light than RuBi-DA but less sensitive than BBHCM-DA, owing to its much larger extinction coefficient. The sensitivity to 2PE of CyHQ-*O*-DA was similar to that of RuBi-DA, the only caged dopamine with a reported 2-photon uncaging action cross-section. BBHCM-DA and CyHQ-*N*-DA have similar photochemical properties and instability toward spontaneous hydrolysis in the dark. Quantitative photochemical data for CNB-, CNV-, and NPEC-DA and stability in the dark for RuBi-DA are not reported, so comparisons to these compounds were not possible.

Hydroxyquinoline PPGs are known to release their payloads on the femto- to nanosecond time scales,[47,51−53] much faster than diffusion through cellular media and dopaminergic signal transduction. We expect CyHQ-*O*-DA to release dopamine with similarly rapid release kinetics, which are on par with those of RuBi-DA.[54] The initial cleavage of the carbamate linkage in CyHQ-*N*-DA would be expected to occur on the same short time scales, but the resulting carbamate decomposes to the free amine on millisecond to second time scales,[36,37] much too slow for tight spatial resolution of dopamine release in cell or tissue slice culture. For the same reason, BBHCM- and NPEC-DA would also release dopamine at a relatively slower rate.

CyHQ-*O*-DA was chosen from among all of the CyHQ-protected dopamine derivatives for biological studies, because it offered the cleanest reaction, best stability in the dark, highest yield of dopamine, fastest release kinetics, and most efficient photolysis at 365 and 405 nm. A 405 nm laser is frequently standard on commercial confocal microscopes (a 365 nm laser is less common), so PPGs that photolyze at this wavelength are desirable probes. CyHQ-sulpiride also possessed the desired photophysical and photochemical properties, solubility, and stability in the dark for physiological use.

Photoactivation of Dopamine in Cell Culture. As an initial test of efficacy, CyHQ-*O*-DA was photolyzed in a culture of MDA-MB-231 cells (a breast cancer line), which express D1

https://dx.doi.org/10.1021/acschemneuro.9b00675
ACS Chem. Neurosci. 2020, 11, 939−951

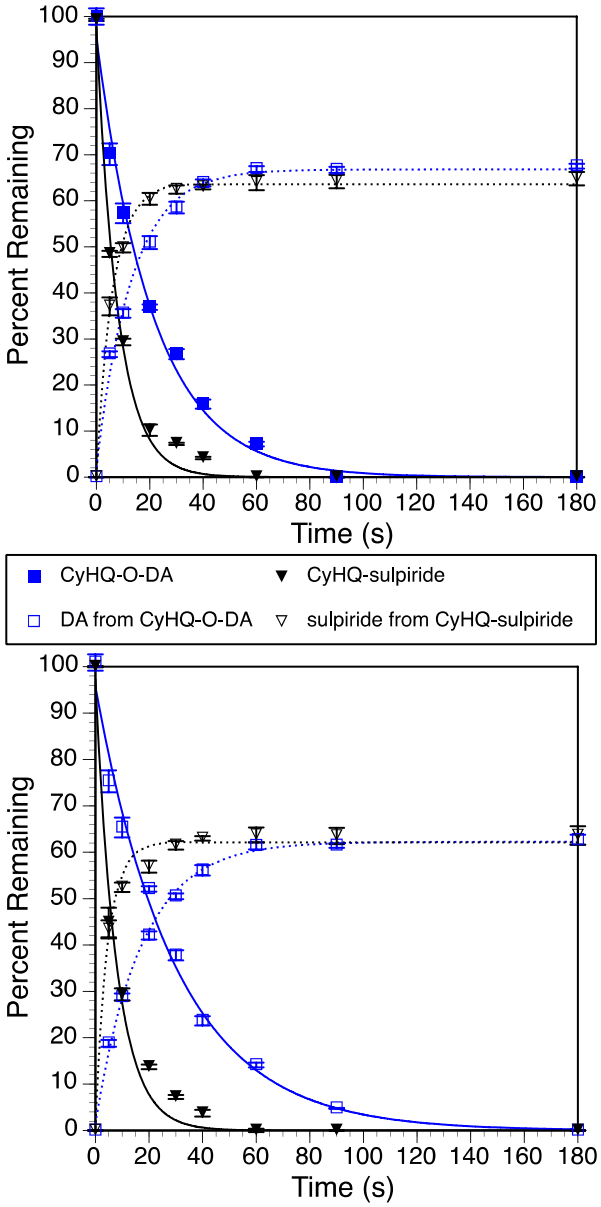

Figure 2. Time courses for the photoreaction of CyHQ-*O*-DA and CyHQ-sulpiride with (top) 365 and (bottom) 405 nm light. Solid lines are the least-squares fit to an exponential decay, and dashed lines are an exponential rise to max for each measurement. Error bars represent the standard deviation of the average of three measurements. See Figures S3 and S4 for time courses of the 1PE-driven photolysis reactions of CyHQ-*N*-DA, $(CyHQ)_2$-*O*,*O*-DA, and $(CyHQ)_2$-*N*,*O*-DA and Figures S5 and S6 for the 2PE-driven photolysis reactions of CyHQ-*O*-DA, $(CyHQ)_2$-*O*,*O*-DA, and CyHQ-sulpiride. See the Supporting Information for representative HPLC traces of the photolysis reactions.

receptors that when activated cause an intracellular $[Ca^{2+}]$ increase.[55,56] Cells were plated on glass-bottom dishes and loaded with the Ca^{2+} indicator Fluo-4 AM. The cells were imaged with a confocal microscope at 488 nm for 800 s to check for aberrant release of dopamine; none was observed. Light from a 405 nm laser (3.8 mW) was applied in close proximity of a cell for 100 ms, and the change in fluorescence intensity across the cell was measured with Fluoview software (Figure 3A, D). In the absence of CyHQ-*O*-DA, no Ca^{2+} signal was observed. When a 1-mM solution of dopamine was added to the MDA-MB-231 cells in culture, a strong Ca^{2+} signal was observed after a delay of more than 200 s (Figure 3B, E). The combination of CyHQ-*O*-DA (1 mM) in the media and a 100 ms pulse of light from the 405 nm laser close to the cell generated a similar signal. Interestingly, a single pulse of light to release dopamine from CyHQ-*O*-DA produced a regular pattern of Ca^{2+} signals in the cells (Figure 3C, F). The dopamine receptor-mediated physiology of these cells is not well-studied, so we are unable ascribe any meaning to this observation.

Photoactivation of Dopamine in Brain Slice. Midbrain dopamine neurons provide an ideal target for testing CyHQ-*O*-DA in acute brain slice. Substantia nigra pars compacta neurons express the inhibitory D2 receptor that activates the G protein-coupled inwardly rectifying potassium (GIRK) channel. These currents can be measured with whole cell voltage clamp recordings to provide a convenient readout of receptor activation. When recirculated over the slice (150 μM, 5 mL), flash photolysis of CyHQ-*O*-DA produced a robust GIRK-mediated outward current with a rapid activation phase and a slow decay (Figure 4). The response increased in amplitude and duration when cocaine was added, as would be expected with an inhibition of dopamine uptake, and all response was blocked with the addition of the D2 receptor antagonist sulpiride (500 nM).

The kinetics of the flash response were compared to synaptically released dopamine and iontophoretically applied dopamine (Figure 5). For medium-strength conditions for photoactivation (2.5 ms of a 1.8 mW pulse, 50 μM CyHQ-*O*-DA), picked because stronger pulses result in slower kinetics, the time the current response took to rise from 10 to 90% of the peak was 210 ms compared with 141 and 270 ms for synaptically released and iontophoretically applied dopamine, respectively. Although only the inhibitory postsynaptic current (IPSC) response was significantly faster than iontophoresis (p = 0.002 one-way ANOVA with Tukey's multiple comparison), the kinetics of the photolysis response represented a middle point between the two (p = 0.08 photolysis vs IPSC, p = 0.13 photolysis vs iontophoresis). The concentration of dopamine sensed by neurons in synaptic release is thought to be quite high (10−30 μM) with lower concentrations producing slower rise-time kinetics.[14] The kinetics of the photolysis response suggests an upper limit in effective dopamine concentration as lower than synaptic, but still in the micromolar range. Comparison to iontophoresis concentration is difficult as iontophoresis pipettes cannot be directly proximal to a neuron.

CyHQ-*O*-DA was tested for any agonism in the absence of photolysis. A concentration−response curve was generated for CyHQ-*O*-DA (Figure 6). CyHQ-*O*-DA did elicit an outward current on its own at higher concentrations but was minimal at working concentrations. The current produced is unlikely to be due to free dopamine as the addition of sulpiride (1 μM) was unable to fully reverse the effect (Figure S7). A low concentration of contaminating free dopamine would be easily blocked by sulpiride, but the data are consistent with a high concentration of a partial agonist competing with sulpiride.

Using a concentration of CyHQ-*O*-DA on the lower end of the concentration−response curve (50 μM), a flash−response curve was generated by sequentially increasing the flash durations and a cocaine concentration to reach maximal response (Figure 7A). Even this lower concentration of CyHQ-*O*-DA was able to effectively saturate the response of the cell with a 100 ms light flash. Note that cocaine itself

https://dx.doi.org/10.1021/acschemneuro.9b00675
ACS Chem. Neurosci. 2020, 11, 939−951

Table 1. Photophysical and Photochemical Properties of CyHQ-, RuBi-, and BBHCM-Protected Dopamine Derivatives and CyHQ-Protected Sulpiride

compound	λ_{max} (nm)	ε_{365} (M^{-1} cm^{-1})	ε_{405} (M^{-1} cm^{-1})	$\Phi_{u(365)}$	$\Phi_{u(405)}$	sensitivity ($\varepsilon_{365}\Phi_u$)	sensitivity ($\varepsilon_{405}\Phi_u$)	yield (%)[d] (365 nm)	yield (%)[d] (405 nm)	δ_u (GM)[b]	dark stability (h)[e]
CyHQ-*O*-DA[a]	365	5300	280	0.19	0.20	990	55	67	61	0.24	100
$(CyHQ)_2$-*O*,*O*-DA[a]	364	5480	324	0.19	0.19	1044	61	16	15	0.12	100
CyHQ-*N*-DA[a]	364	6700	251	0.19	0.20	1283	50	60	49	n.p.[c]	24
$(CyHQ)_2$-*N*,*O*-DA[a]	364	8300	631	0.02	0.018	142	11	4	2	n.p.[c]	24
CyHQ-sulpiride[a]	372	6500	830	0.19	0.22	1239	184	65	63	0.26	72
RuBi-DA[25]	447		4900 (447 nm)		0.085		420 (447 nm)			0.24[f]	
BBHCM-DA[26]	372	18 000 (372 nm)		0.12		2160 (372 nm)					7% loss in 24 h

[a]0.1 mM solution in KMOPS buffer, pH 7.2. [b]Excitation at 740 nm, M = 10^{-50} cm^4 s/photon. [c]No photolysis. [d]Yield of DA or sulpiride measured by HPLC. [e]No spontaneous hydrolysis in the dark observed within the time given. [f]Excitation at 800 nm. See Tables S1 and S2 for the data used to calculate Φ_u and δ_u.

produced a small current due to spontaneously released dopamine that is no longer being transported, which is consistent with cocaine-induced cell behavior in the absence of CyHQ-*O*-DA.[57] This current was included in the calculation of maximum response. To test for stability over time, CyHQ-*O*-DA was photolyzed once per minute with a 10 ms flash, which gave a half-maximal response in the flash-response experiment, for 15 min with no appreciable decline in response (Figure 7B). This indicates that a relatively small proportion of CyHQ-*O*-DA in the 5 mL of recirculating solution was photolyzed to produce the half-maximal response. This suggests that longer experiments can be feasible particularly with larger recirculation volumes.

Photoactivation of Sulpiride in Brain Slice. One of the uses for a caged antagonist is to probe the dissociation rates of agonists by measuring the decay constants of receptor signaling following photolysis. To test the properties of CyHQ-sulpiride with dopamine neurons, dopamine (1 μM) or quinpirole (300 nM) was recirculated to activate D2 receptors. Following the period of initial application, CyHQ-sulpiride (5 μM) was added, which induced a small reduction in the D2 receptor dependent current, indicating a small amount of antagonism for the still-caged sulpiride (Figure S8). For initial tests, CyHQ-sulpiride was photolyzed with a long flash (1 s) from and LED (6.5 mW) (Figure 8). The time constant of decay for quinpirole (τ = 635 ms) was significantly slower than that of dopamine (τ = 307 ms), which dissociates faster (k_{off} = 1.69 min^{-1})[58] than quinpirole (k_{off} = 0.17 min^{-1})[59] (p = 0.0011 by t test, n = 4 and 2 for quinpirole and dopamine, respectively). The amplitude of the peak response of the agonists were not significantly different, so cannot be considered a confounding factor.

To enable more precise experiments such as those used for studying dopamine synaptic biology, we tested the ability of CyHQ-sulpiride to mediate D2 receptor signaling under more stringent conditions. A single 50 ms light pulse while CyHQ-sulpiride (5 μM) recirculates through the slice preparation is sufficient to block the dopamine IPSC, consisting of a 10−30 μM local concentration of dopamine near the receptors (Figure 9). This result and the previously observed kinetics of the block on the standing currents suggest CyHQ-sulpiride can be used to probe dopamine synaptic release and receptor signaling with fine temporal precision.

CONCLUSION

Several photoactivatable forms of dopamine and the D2 receptor antagonist sulpiride were designed, synthesized, and tested for their ability to release their respective payloads through 1PE and 2PE processes. From among the dopamine derivatives prepared in this study, CyHQ-*O*-DA possessed the best photochemical properties, releasing dopamine with a quantum yield of 19−20%, a chemical yield of 61−67%, high sensitivity to 1PE, and modest sensitivity to 2PE. CyHQ-sulpiride exhibited similar 1PE- and 2PE-mediated photochemical properties. Importantly, both compounds were extremely stable in neutral aqueous buffer in the dark and could release their payloads at 405 nm, a laser wavelength typically included in commercially available confocal microscopes. CyHQ-*O*-DA mediated the activation of D1 receptors on MDA-MB-231 cells in culture with 405 nm light. In brain slice from the substantia nigra pars compacta, CyHQ-*O*-DA mediated the light activation of D2 receptors on dopamine neurons that closely mimicked the natural action of dopamine on neurons. The D2 receptor activation from released dopamine was light-dose dependent, and repeated photoactivation could be executed without deterioration of the response, indicating that experiments of long duration are possible with this tool. CyHQ-sulpiride had minimal background activity and photolyzed efficiently to rapidly antagonize D2 receptors and enable the measurement of agonist off rates and other elements of dopamine synapse physiology. These tools will enable more detailed study of dopamine receptors, their interactions with other GPCRs, and the physiology of dopamine signaling in the brain.

EXPERIMENTAL SECTION

Synthesis. *General.* Reagents and solvents were purchased from commercially readily available sources and utilized without any further purification. Bruker Avance III HD 500 or 600 MHz NMR spectrometer was used to record the ^{1}H NMR and ^{13}C NMR spectra. UV−vis spectra were recorded on a Cary 5000 UV−vis−NIR spectrophotometer (Agilent). An Agilent Infinity series system with an autosampler and diode array detector was used for HPLC and

https://dx.doi.org/10.1021/acschemneuro.9b00675
ACS Chem. Neurosci. 2020, 11, 939−951

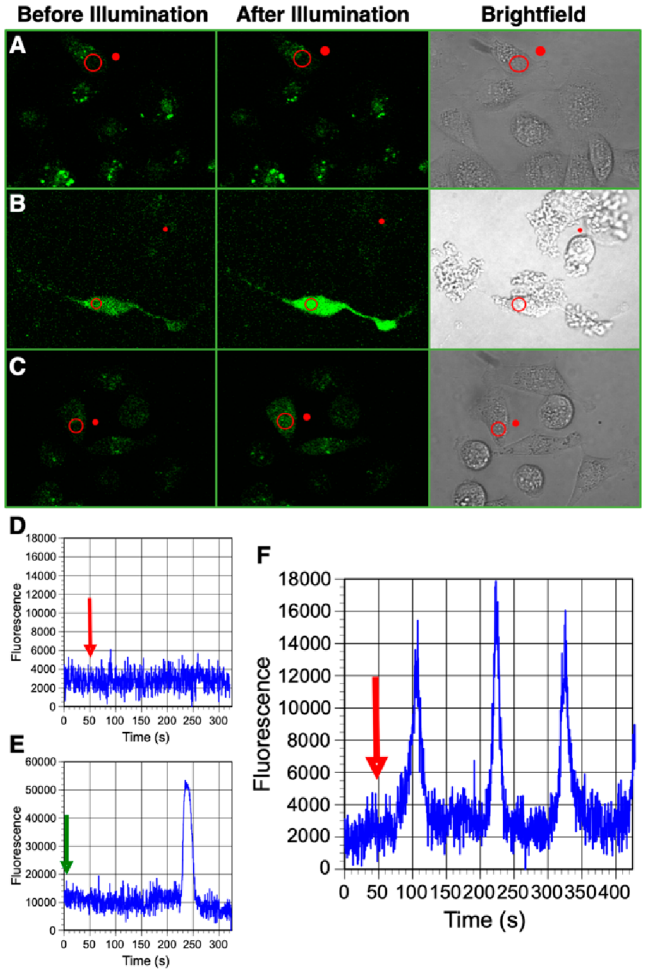

Figure 3. Activation of D1 receptors on MDA-MB-231 cells with 405 nm light. Solid red circle indicates point of illumination or location of addition of dopamine (1 mM); open red circle indicates position of fluorescence intensity measurement. Red arrow indicates time of illumination with a 100 ms pulse of 405 nm light. Green arrow indicates time of dopamine addition. (A) Confocal microscopy image of fluorescence output from Fluo-4 before (left) and after (middle) illumination and (right) brightfield image in the absence of dopamine and CyHQ-*O*-DA. (B) Confocal microscopy image of fluorescence output from Fluo-4 before (left) and after (middle) addition of dopamine (1 mM) and (right) brightfield image. (C) Confocal microscopy image of fluorescence output from Fluo-4 before (left) and after (middle) illumination and (right) brightfield image in the presence of CyHQ-*O*-DA (1 mM). (D) Fluorescence intensity observed over time in the absence of dopamine and CyHQ-*O*-DA. (E) Fluorescence intensity observed over time with addition of dopamine (1 mM). (F) Fluorescence intensity observed over time in the presence of CyHQ-*O*-DA (1 mM).

uHPLC (preparative and analytical) with Zorbax eclipse C-18 reverse phase columns. An Agilent 6540 HD Accurate Mass QTOF/LC-MS with ESI or a Micromass QTOF-Ultima with ESI was used for recording HRMS. KMOPS buffer was made from 100 mM KCl and 10 mM MOPS titrated to pH 7.2 with KOH. Flash chromatography was performed on an Isolera Spektra 4 with Biotage SNAP cartridges packed with KPSIL silica.

tert-Butyl (3-((8-Cyano-7-(methoxymethoxy)quinolin-2-yl)-methoxy)-4-hydroxyphenethyl)carbamate and tert-Butyl (4-((8-Cyano-7-(methoxymethoxy)quinolin-2-yl)methoxy)-3-hydroxyphenethyl)carbamate (MOM-CyHQ-O-DA-Boc). MOM-CyHQ-OMs (0.50 g, 1.54 mmol) was dissolved in acetone (20 mL). To the resulting solution, Boc-protected dopamine (0.39 g, 1.54 mmol) was added followed by cesium carbonate (1.00 g, 3.08 mmol). The mixture was stirred at room temperature and monitored by uHPLC until completion. The mixture was concentrated under vacuum, and the resulting residue was purified over silica gel, eluting with EtOAc/hexanes (2:3) to yield MOM-CyHQ-O−DA-Boc (mixture of regioisomers) as a yellow oil (0.48 g, 65%): ^{1}H NMR (600 MHz, chloroform-*d*, δ) 8.23−8.10 (m, 1H), 7.99 (d, J = 9.2 Hz, 1H), 7.73 (d, J = 8.4 Hz, 1H), 7.57 (d, J = 9.2 Hz, 1H), 7.15−6.67 (m, 3H), 5.73−5.23 (m, 4H), 3.61 (d, J = 0.9 Hz, 3H), 3.38−3.29 (m, 2H), 2.83−2.60 (m, 2H), 1.45 (s, 9H). ^{13}C NMR (151 MHz, methanol-d_4, δ) 167.5, 162.1, 147.0, 145.3, 145.1, 144.2, 141.2, 135.4, 127.7, 122.6, 119.9, 119.6, 117.5, 115.4, 115.3, 112.0, 97.0, 89.1, 85.0, 60.9, 53.9, 40.8, 32.6, 26.2; HRMS (ESI-QTOF) m/z: [M + H]$^+$ calcd for $C_{26}H_{29}N_3O_6$, 480.2129; found, 480.2130.

2-(4-((8-Cyano-7-hydroxyquinolin-2-yl)methoxy)-3-hydroxyphenyl)ethan-1-aminium 2,2,2-trifluoroacetate and 2-(3-((8-Cyano-7-hydroxyquinolin-2-yl)methoxy)-4-hydroxyphenyl)-ethan-1-aminium 2,2,2-trifluoroacetate (CyHQ-O-DA). MOM-CyHQ-O−DA-Boc (0.50 g, 1.04 mmol) was dissolved in 1:1 CH_2Cl_2/TFA (10 mL), and the mixture was stirred for 12 h in the dark. The progress of the reaction was monitored by LCMS. Upon complete consumption of the starting materials, the solvents were evaporated. The resulting residue was purified by preparative HPLC, eluting with a gradient of A and B, where A = 0.1% TFA in water and B = acetonitrile. The gradient started with 100% A and 0% B and finished with 0% A and 100% B in 12 min to yield the TFA salt of CyHQ-*O*-DA (10:7 mixture of regioisomers) as a residue on the flask wall (0.40 g, 85%): Isomer 1: ^{1}H NMR (500 MHz, methanol-d_4, δ) 8.30 (d, J = 8.4 Hz, 1H), 8.05 (d, J = 9.1 Hz, 1H), 7.71 (d, J = 8.4 Hz, 1H), 7.30 (d, J = 9.1 Hz, 2H), 7.08 (d, J = 2.0 Hz, 1H), 6.85 (d, J = 8.1 Hz, 1H), 6.75 (dd, J = 8.1, 2.0 Hz, 1H), 5.47 (s, 2H), 3.16−3.08 (m, 2H), 2.83 (t, J = 7.8 Hz, 2H); ^{13}C NMR (126 MHz, methanol-d_4, δ) 164.3, 160.4, 146.7, 146.0, 145.7, 137.4, 134.0, 133.9, 130.2, 127.7, 121.9, 121.8, 119.5, 118.1, 117.8, 115.9, 114.6, 114.5, 71.6, 40.7, 32.7; Isomer 2: ^{1}H NMR (500 MHz, methanol-d_4, δ) 8.28 (d, J = 8.5 Hz, 1H), 8.04 (d, J = 8.9 Hz, 1H), 7.67 (d, J = 8.4 Hz, 1H), 7.30 (d, J = 9.1 Hz, 2H), 7.02 (d, J = 8.2 Hz, 1H), 6.81 (d, J = 2.1 Hz, 1H), 6.67 (dd, J = 8.3, 2.2 Hz, 1H), 5.44 (s, 2H), 3.16−3.08 (m, 2H), 2.84 (t, J

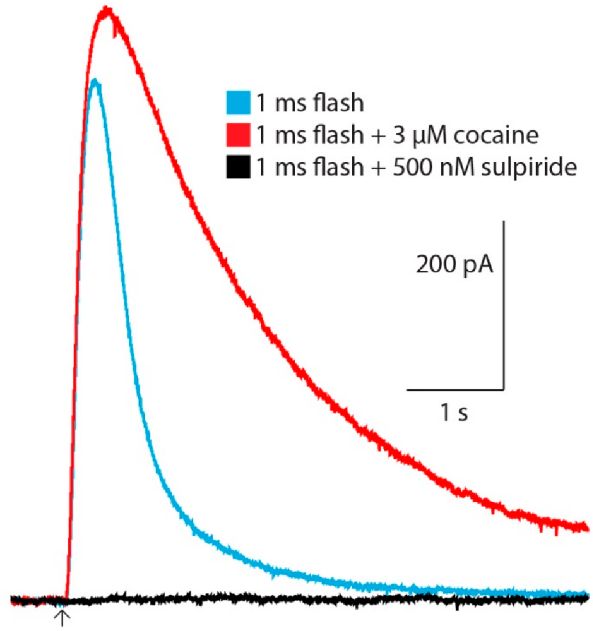

Figure 4. Activation of D2 receptors on substantia nigra dopamine neurons with 365 nm light. Blue arrow indicates point of 1 ms flash. In blue is the response with CyHQ-*O*-DA (150 μM), in red is the response after the addition of cocaine (3 μM) to inhibit dopamine transport, and in black is the response after D2 receptors were blocked with sulpiride (500 nM).

https://dx.doi.org/10.1021/acschemneuro.9b00675
ACS Chem. Neurosci. 2020, 11, 939−951

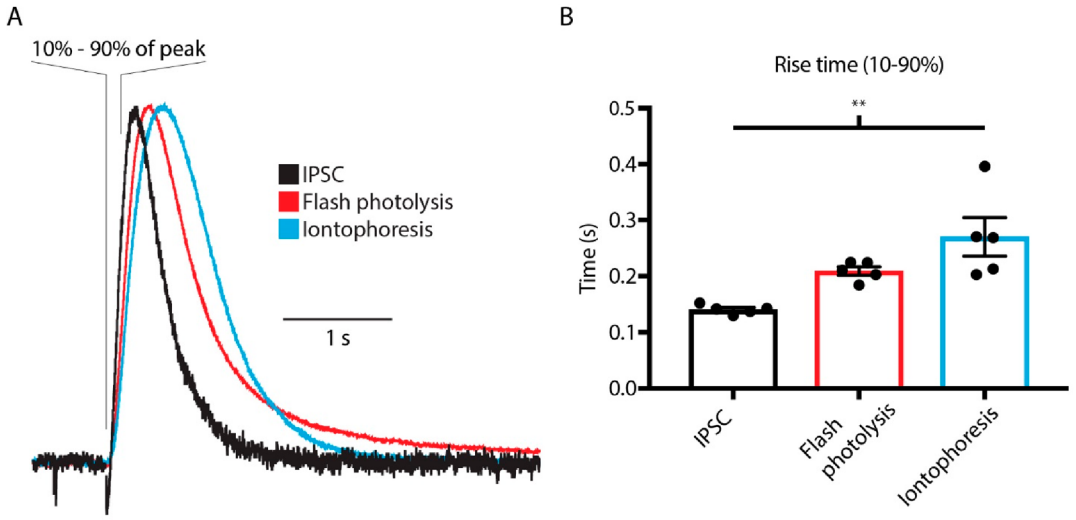

Figure 5. Kinetic comparison of normalized dopamine responses. (A) Scaled responses to flash photolysis (2.5 ms, 1.8 mW) of CyHQ-*O*-DA (50 μM), electrically stimulated dopamine IPSC (single stimulation), and dopamine iontophoresis (1 M dopamine, 4 nA backing current, 10 ms of a 100 nA ejection pulse). (B) Rise times from 10 to 90% of peak current as outlined in A. There was a gradient of speed with the IPSC response being the fastest, then flash photolysis, then iontophoresis. Though only the IPSC response was significantly faster than iontophoresis (one-way ANOVA with Tukey's multiple comparison), the kinetics of the photolysis response were on the edge of significance on both ends (p = 0.08 vs IPSC, p = 0.13 vs iontophoresis).

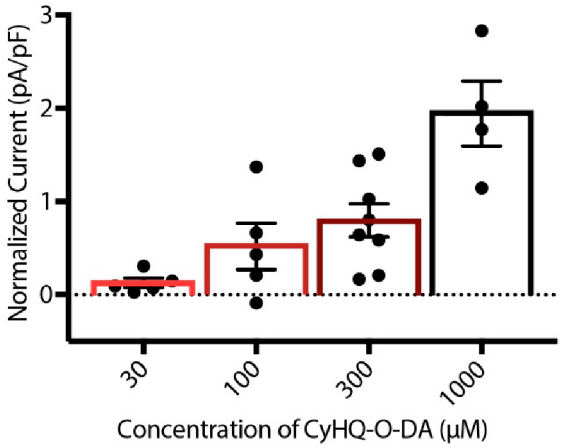

Figure 6. Concentration−response curve for CyHQ-*O*-DA applied to dopamine neurons in the absence of photolysis. The current generated from adding CyHQ-*O*-DA was measured and normalized to the size of the cell as measured by capacitance in picofarads (pF).

= 7.7 Hz, 2H); ^{13}C NMR (126 MHz, methanol-d_4, δ) 164.3, 160.5, 146.7, 146.0, 145.7, 137.3, 134.0, 133.9, 130.2, 127.7, 121.9, 121.8, 119.5, 117.8, 117.7, 116.0, 114.9, 114.7, 71.6, 40.7, 32.7; HRMS (ESI-QTOF) m/z: [M + H]$^+$ calcd for $C_{19}H_{17}N_3O_3$, 336.1343; found, 336.1347.

2,2′-(((4-(2-Aminoethyl)-1,2-phenylene)bis(oxy))bis(methylene))-bis(7-hydroxyquinoline-8-carbonitrile) ((CyHQ)$_2$-O,O-DA). MOM-CyHQ-OMs (0.01 g, 0.03 mmol) was dissolved in acetone (1 mL) followed by the addition of cesium carbonate (0.02 g, 0.06 mmol) and *tert*-butyl (3,4-dihydroxyphenethyl)carbamate (0.004 g, 0.016 mmol). The mixture was stirred for 24 h, after which time the acetone was evaporated and the remaining residue dissolved in ethyl acetate (10 mL). The solution was washed with water (10 mL), dried over magnesium sulfate, filtered, and evaporated. The resulting residue was dissolved in methanol (2 mL), and TMSCl (0.012 mL, 0.093 mmol) was added to the solution, followed by stirring overnight. The solvent was evaporated, and the remaining residue was purified by preparative HPLC, eluting with a gradient of A and B, where A = 0.1% TFA in water and B = acetonitrile. The gradient started with 100% A and 0% B and finished with 0% A and 100% B in 12 min to yield (CyHQ)$_2$-*O*,*O*-DA as its TFA salt (0.008 g, 45% over two steps): ^{1}H NMR (500 MHz, methanol-d_4, δ) 8.17 (dd, J = 8.4, 4.2 Hz, 2H), 7.92 (dd, J = 9.0, 3.7 Hz, 2H), 7.64 (dd, J = 8.4, 7.2 Hz, 2H), 7.20 (dd, J = 9.1, 3.2 Hz, 2H), 7.15−7.11 (m, 1H), 7.07 (d, J = 8.2 Hz, 1H), 6.80 (dd, J = 8.2, 2.0 Hz, 1H), 5.40 (s, 2H), 5.36 (s, 2H), 3.10 (dd, J = 8.4, 6.9 Hz, 2H), 2.83 (t, J = 7.6 Hz, 2H); ^{13}C NMR (126 MHz, methanol-d_4, δ) 164.2, 164.2, 160.4, 160.2, 149.0, 148.4, 147.8, 137.3, 137.2, 137.1, 134.0, 133.9, 133.8, 130.3, 130.2, 122.0, 121.6, 118.0, 117.8, 117.7, 117.6, 115.5, 114.8, 94.3, 94.2, 94.1, 72.1, 72.0, 40.5, 32.6; HRMS (ESI-QTOF) m/z: [M + H]$^+$ calculated for $C_{28}H_{23}N_5O_4$, 518.1823; found, 518.1826.

(8-Cyano-7-(methoxymethoxy)quinolin-2-yl)methyl(3,4-dihydroxyphenethyl)carbamate (MOM-CyHQ-N-DA). MOM-CyHQ−OH (0.1 g, 0.41 mmol) was dissolved in CH_2Cl_2 (10 mL). To the resulting solution, 1,1′-carbonyldiimidazole (0.265 g, 1.64 mmol) was added, and the reaction was stirred until the starting material was completely consumed, as indicated by LCMS analysis. The solution was washed with water (5 mL) and dried with $MgSO_4$, followed by evaporation of the solvent. The resulting residue was dissolved in DMF (5 mL). In a separate flask, triethylamine (1 mL) was added to a solution of dopamine·HCl (0.46 g, 2.45 mmol) in DMF (5 mL). The resulting white precipitate dissolved after a few minutes of stirring. After 30 min of stirring, the previously prepared CyHQ-CDI intermediate was added, and the resulting mixture was stirred for 6 h or until LCMS analysis indicated the complete consumption of starting materials. The DMF was evaporated, and the resulting residue was dissolved in ethyl acetate (50 mL). The solution was washed with water (30 mL) and evaporated, and the remaining residue was purified by column chromatography (1:1 ethyl acetate/hexane) to give MOM-CyHQ-*N*-DA (0.11 g, 65%): ^{1}H NMR (500 MHz, chloroform-*d*, δ) 8.10 (d, J = 8.4 Hz, 1H), 8.01 (s, 1H), 7.94 (d, J = 9.2 Hz, 1H), 7.50 (d, J = 9.2 Hz, 1H), 7.33 (d, J = 8.5 Hz, 1H), 6.82−6.79 (m, 1H), 6.59−6.53 (m, 1H), 5.44 (s, 2H), 5.38 (s, 2H), 3.57 (s, 3H), 3.43 (q, J = 6.3 Hz, 2H), 2.68 (t, J = 6.5 Hz, 2H); ^{13}C NMR (126 MHz, chloroform-*d*, δ) 162.8, 160.3, 156.3, 148.2, 144.1, 143.1, 136.9, 133.9, 130.8, 122.7, 120.7, 118.6, 115.8, 115.5, 115.24, 114.5, 99.2, 95.1, 66.7, 56.9, 42.4, 35.3; HRMS (ESI-QTOF) m/z: [M + H]$^+$ calculated for $C_{22}H_{21}N_3O_6$, 424.1509; found, 424.1515.

(8-Cyano-7-hydroxyquinolin-2-yl)methyl(3,4-dihydroxyphenethyl)carbamate (CyHQ-N-DA). MOM-CyHQ-*N*-DA (0.10 g, 0.24 mmol) was dissolved in 1:1 CH_2Cl_2/TFA (2 mL), and

https://dx.doi.org/10.1021/acschemneuro.9b00675
ACS Chem. Neurosci. 2020, 11, 939−951

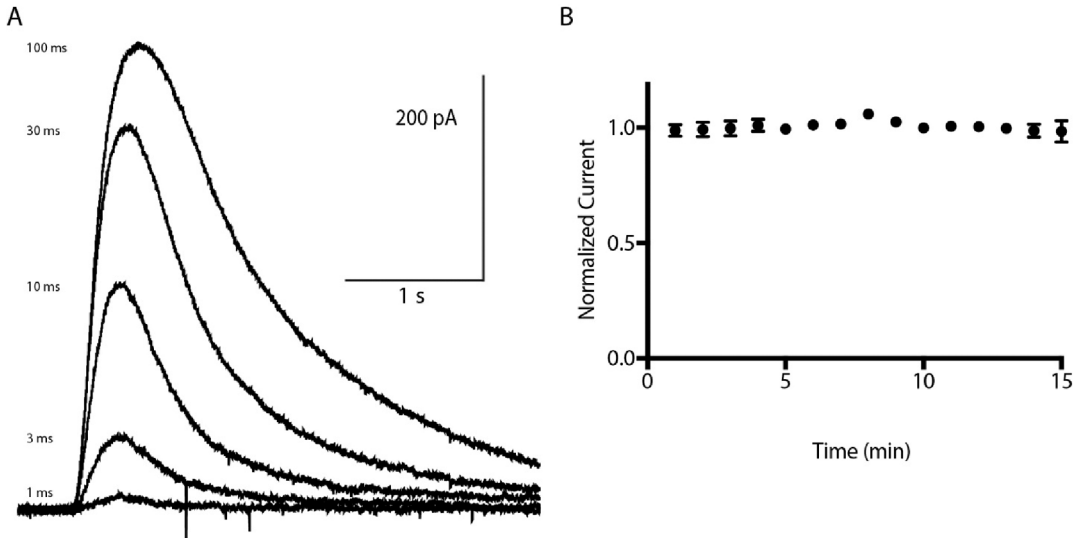

Figure 7. CyHQ-*O*-DA is effective at low concentrations. (A) Electrophysiological response of CyHQ-*O*-DA (50 μM) when photolyzed by flashes of increased duration. (B) Electrophysiological response from repeated photolysis of CyHQ-*O*-DA (50 μM) with 10 ms light flashes every minute.

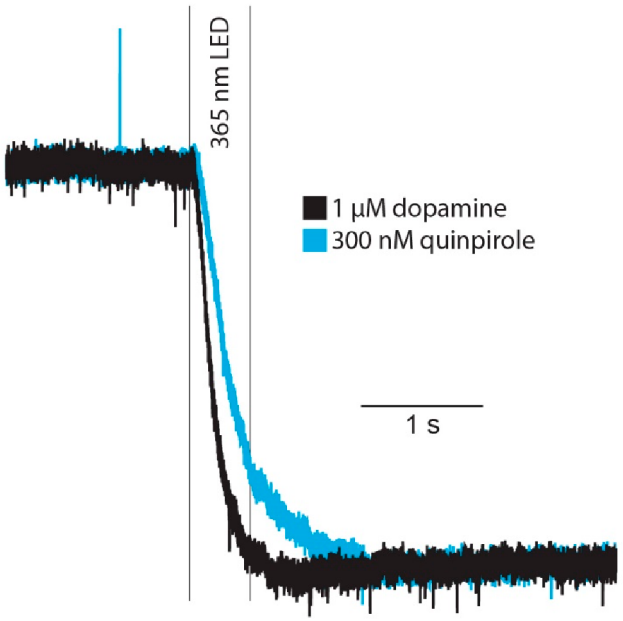

Figure 8. Photolysis of CyHQ-sulpiride can rapidly antagonize D2 receptors. Representative traces of the effects of CyHQ-sulpiride photolysis on currents produced by the D2 receptor activated by quinpirole (300 nM) or dopamine (1 μM, currents have been scaled for better comparison of kinetics). The rate of decline for quinpirole was significantly slower for quinpirole than for dopamine (p = 0.0011, τ = 635 and 307 ms, n = 4 and 2 for quinpirole and dopamine, respectively).

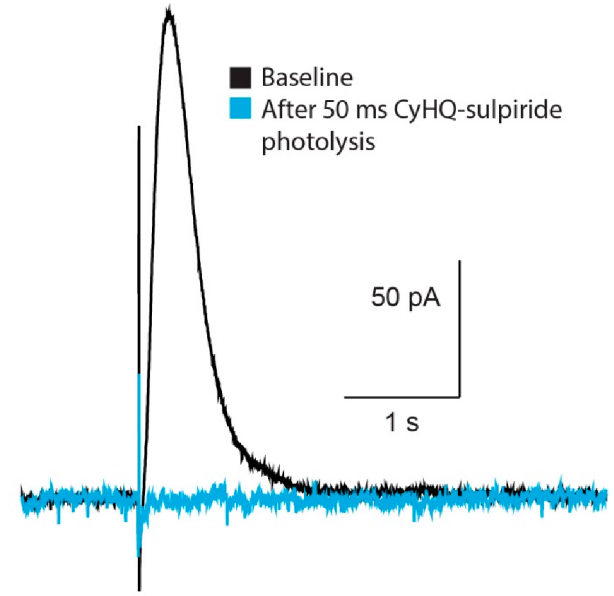

Figure 9. Short light pulses and CyHQ-sulpiride are effective at blocking synaptic activity. The baseline IPSC with CyHQ-sulpiride (5 μM) recirculating over the slice is shown in black. The blue trace shows the complete block of the dopamine IPSC elicited 1 min after a single 50 ms flash of 365 nm light from an LED.

the mixture was stirred for 6 h in the dark or LCMS analysis indicated the complete consumption of starting material. The solvents were evaporated under vacuum, and the resulting residue was purified over silica gel, eluting with EtOAc/hexanes (2:1) to yield CyHQ-*N*-DA as a brownish solid (0.063 g, 70%): ^{1}H NMR (500 MHz, methanol-d_4, δ) 8.23 (d, J = 8.4 Hz, 1H), 7.98 (d, J = 9.0 Hz, 1H), 7.34 (d, J = 8.4 Hz, 1H), 7.24 (d, J = 9.0 Hz, 1H), 6.73−6.66 (m, 2H), 6.56 (dd, J = 8.0, 2.1 Hz, 1H), 5.34 (s, 2H), 3.36 (d, J = 7.2 Hz, 2H), 2.69 (t, J = 7.3 Hz, 2H); ^{13}C NMR (126 MHz, methanol-d_4, δ) 164.1, 160.1, 157.1, 148.2, 144.8, 143.3, 137.3, 133.8, 130.6, 121.5, 119.8, 117.5, 116.9, 115.6, 115.0, 114.7, 94.2, 66.4, 42.3, 35.1; HRMS (ESI-QTOF) m/z: [M + H]$^+$ calculated for $C_{20}H_{17}N_3O_5$, 380.1241; found, 380.1249.

(8-Cyano-7-hydroxyquinolin-2-yl)methyl(3-((8-cyano-7-hydroxyquinolin-2-yl)methoxy)-3-hydroxyphenethyl)carbamate and (8-Cyano-7-hydroxyquinolin-2-yl)methyl(4-((8-cyano-7-hydroxyquinolin-2-yl)methoxy)-3-hydroxyphenethyl)carbamate ((CyHQ)$_2$-N,O-DA). MOM-CyHQ-*N*-DA (0.02 g, 0.047 mmol) was dissolved acetone (2 mL) followed by the addition of cesium carbonate (0.03 g, 0.094 mmol) and MOM-CyHQ-OMs (0.015 g, 0.047 mmol). The mixture stirred for 24 h, after which time the acetone was evaporated and the remaining residue dissolved in ethyl acetate (20 mL). The solution was washed with water (10 mL), dried over magnesium sulfate, filtered, and evaporated. The resulting residue was dissolved in methanol (2 mL), and TMSCl (0.02 mL, 0.141 mmol) was added to the solution, followed by stirring overnight. The solvent was evaporated, and the remaining residue was purified through reverse

https://dx.doi.org/10.1021/acschemneuro.9b00675
ACS Chem. Neurosci. 2020, 11, 939−951

phase column chromatography utilizing a gradient of A and B, where A = 0.1% TFA in water and B = acetonitrile. The gradient started with 100% A and 0% B and finished with 0% A and 100% B in 12 min to give the two regioisomers of $(CyHQ)_2$-*N*,*O*-DA in a 2:1 ratio (0.006 g, 21% over two steps): Isomer 1: ^{1}H NMR (500 MHz, methanol-d_4, δ) 8.15 (dd, J = 12.7, 8.4 Hz, 2H), 7.92 (t, J = 9.2 Hz, 2H), 7.58 (d, J = 8.4 Hz, 1H), 7.26−7.16 (m, 2H), 7.12 (d, J = 8.4 Hz, 1H), 7.01 (d, J = 1.9 Hz, 1H), 6.85−6.77 (m, 1H), 6.74 (dd, J = 8.1, 1.9 Hz, 1H), 5.39 (s, 2H), 5.26 (s, 2H), 3.37 (t, J = 6.7 Hz, 2H), 2.72 (t, J = 7.1 Hz, 2H); ^{13}C NMR (126 MHz, methanol-d_4, δ) 164.2, 164.1, 164.0, 160.4, 160.1, 157.0, 148.4, 148.2, 146.7, 145.2, 137.2, 137.1, 133.9, 133.8, 130.7, 122.3, 121.5, 121.4, 119.8, 117.9, 117.4, 116.9, 116.7, 115.5, 115.2, 94.2, 94.1, 71.8, 66.3, 42.1, 35.0; Isomer 2: ^{1}H NMR (500 MHz, methanol-d_4, δ) 8.22 (d, J = 8.4 Hz, 2H), 7.98 (d, J = 9.1 Hz, 2H), 7.63 (d, J = 8.3 Hz, 1H), 7.34−7.29 (m, 1H), 7.26−7.16 (m, 2H), 6.93 (d, J = 8.2 Hz, 1H), 6.85−6.77 (m, 1H), 6.64 (dd, J = 8.3, 2.1 Hz, 1H), 5.41 (s, 2H), 5.30 (s, 2H), 3.37 (t, J = 6.7 Hz, 2H), 2.72 (t, J = 7.1 Hz, 2H). ^{13}C NMR (126 MHz, methanol-d_4, δ) 164.2, 164.1, 164.0, 160.7, 160.0, 157.0, 148.3, 148.2, 146.3, 144.9, 137.2, 137.1, 133.9, 133.8, 130.7, 122.3, 121.7, 121.6, 119.8, 117.5, 117.4, 116.3, 114.8, 114.7, 114.2, 94.2, 94.1, 71.8, 66.3, 42.0, 35.1; HRMS (ESI-QTOF) m/z: $[M + H]^+$ calcd for $C_{31}H_{23}N_5O_6$ 562.1726; found 562.1729.

1-((8-Cyano-7-hydroxyquinolin-2-yl)methyl)-1-ethyl-2-((2-methoxy-5-sulfamoylbenzamido)methyl)pyrrolidin-1-ium (CyHQ-Sulpiride) 2,2,2-Trifluoroacetate. MOM-CyHQ-OMs (0.50 g, 1.54 mmol) was dissolved in acetonitrile (10 mL), and sulpiride (0.53 g, 1.54 mmol) was added. The resulting solution was heated at reflux overnight or LCMS analysis indicated the complete consumption of starting material. The solvent was evaporated and the remaining residue was taken up in 1:1 mixture of TFA/CH_2Cl_2 (10 mL) and water (50 μL) followed by stirring overnight. The solvents were evaporated, and the remaining residue was purified over silica gel, eluting with EtOAc to yield the TFA salt of CyHQ-sulpiride as a brown solid (0.69 g, 70%): Diastereomer 1: ^{1}H NMR (500 MHz, methanol-d_4, δ) 8.39 (d, J = 8.3 Hz, 1H), 8.35 (d, J = 2.5 Hz, 1H), 8.08 (d, J = 9.1 Hz, 1H), 8.01 (dd, J = 8.8, 2.5 Hz, 1H), 7.60 (d, J = 8.3 Hz, 1H), 7.37 (d, J = 9.0 Hz, 1H), 7.27 (d, J = 8.9 Hz, 1H), 5.09 (d, J = 15.1 Hz, 1H), 4.97 (d, J = 15.1 Hz, 1H), 4.65 (q, J = 6.7 Hz, 1H), 4.27 (dd, J = 14.5, 6.4 Hz, 1H), 4.05 (s, 3H), 4.04−3.93 (m, 3H), 3.89−3.80 (m, 1H), 3.76 (dq, J = 14.1, 7.2 Hz, 1H), 2.59 (ddd, J = 17.7, 8.5, 4.9 Hz, 1H), 2.47−2.15 (m, 3H), 1.43 (t, J = 7.2 Hz, 3H); ^{13}C NMR (126 MHz, methanol-d_4, δ) 165.9, 159.9, 155.9, 152.4, 148.9, 146.7, 138.3, 136.2, 133.9, 131.0, 129.1, 121.8, 121.5, 120.6, 119.4, 115.1, 111.9, 72.7, 60.1, 57.6, 55.8, 48.2, 48.0, 47.9, 38.8, 25.8, 18.7, 7.4; Diastereomer 2: ^{1}H NMR (500 MHz, methanol-d_4, δ) 8.31 (d, J = 8.2 Hz, 1H), 8.23 (d, J = 2.5 Hz, 1H), 7.99−7.91 (m, 2H), 7.60 (d, J = 8.2 Hz, 1H), 7.23 (d, J = 9.1 Hz, 1H), 7.18 (d, J = 8.8 Hz, 1H), 5.09 (d, J = 15.1 Hz, 1H), 4.97 (d, J = 15.1 Hz, 1H), 4.70−4.62 (m, 1H), 4.22−4.10 (m, 1H), 4.05 (s, 3H), 4.03−3.94 (m, 3H), 3.73−3.57 (m, 2H), 2.40−2.19 (m, 3H), 2.19−2.10 (m, 1H), 1.51 (t, J = 7.2 Hz, 3H). ^{13}C NMR (126 MHz, methanol-d_4, δ) 165.33, 159.88, 152.5, 151.8, 148.9, 140.4, 138.3, 136.2, 133.9, 131.0, 129.3, 122.0, 120.6, 119.4, 117.9, 117.8, 111.8, 72.6, 62.8, 61.2, 55.8, 48.2, 48.0, 48.0, 38.5, 27.2, 19.9, 8.2; HRMS (ESI-QTOF) m/z: $[M - CF_3CO_2]^+$ calcd for $C_{28}H_{30}N_5O_7S$ 524.1962; found 524.1964.

Photochemistry. The photochemical properties of the CyHQ-protected dopamine derivatives and sulpiride (Φ_u, chemical yield, δ_u, and stability in the dark) were measured as previously described.[45,47,60,61]

Cell Culture. MDA-MB-231 cells were cultured in DMEM with 10% FBS and 1% penicillin/streptomycin in cell culture flasks at 37 °C and 5% CO_2.

Calcium Dye Loading into Cells in Culture. MDA-MB-231 cells were plated on a 35 mm glass bottom dish 1 day prior to the microscopy experiment. Calcium dye (50 μg, Fluo-4 AM, Life Technologies) was dissolved in DMSO (50 μL). Both Fluo-4 AM and Pluronic F-127 (Molecular Probes) were added to HBSS resulting in a 0.002% final concentration of each. The mixture was sonicated for 5 min, loaded onto cells growing in a 35 mm glass bottom dish, and then de-esterified for 30 min in a humidified CO_2 incubator (37 °C, 5% CO_2). The cell culture media was replaced with HBSS (1.26 mM $CaCl_2$ and 0.5 mM $MgCl_2{\cdot}6H_2O$) and Ca^{2+} influx experiments were carried out.

Activation of Dopamine Receptors on Cells in Culture. Live cell imaging of the MDA-MB-231 cells loaded with Fluo-4 was carried out on an Olympus FluoView FV1000MPE confocal microscope using a 40× objective (Olympus UPLSAPO40X2, NA 0.95). Fluo-4 was excited by an argon ion laser at 488 nm and emitted light was reflected through a 500−600 nm filter from a dichroic mirror. Data capture and extraction was carried out with FluoView 10-ASW version 4.0 (Olympus), ImageJ-Fiji, and DeltaGraph (Red Rock Software). Stock solutions (25 mM) of dopamine and CyHQ-*O*-DA were prepared in water and kept in the dark prior to and during use. To initiate the experiments, dopamine (1 mM final concentration) was added to the culture dish from a pipet or CyHQ-*O*-DA (1 mM final concentration) was added to the culture dish from a pipet followed by a 100 ms flash of light from the 405 nm laser directed near a cell.

Slice Electrophysiology. Mice, maintained according to approved protocols at Oregon Health and Science University, were deeply anesthetized with isoflurane and killed by decapitation. Male and female C57BL/6J mice between the ages of 60 to 90 days were used. Brains were removed and placed in warm (30 °C) physiologically equivalent saline solution (modified Krebs buffer) containing NaCl (126 mM), KCl (2.5 mM), $MgCl_2$ (1.2 mM), $CaCl_2$ (2.4 mM), NaH_2PO_4 (1.4 mM), $NaHCO_3$ (25 mM), and D-glucose (11 mM) with MK-801 (3 μM), and cut horizontally (222 μm) using a vibrating microtome (Leica). Slices recovered at 30 °C in vials with 95/5% O_2/CO_2 saline with MK801 (10 μM) for at least 30 min prior to recording. Slices were mounted in the recording chamber of an upright microscope (Olympus). The temperature was maintained at 34−36 °C, and modified Krebs buffer was perfused over the slices at 1−2 mL/min. Recordings were obtained with large glass electrodes with a resistance of 1.3−1.9 MΩ when filled with an internal solution containing potassium methanesulfonate (75 mM), NaCl (20 mM), $MgCl_2$ (1.5 mM), HEPES potassium salt (5 mM), ATP (2 mM), GTP (0.2 mM), phosphocreatine (10 mM), and BAPTA tetrapotassium salt pH 7.35−7.45 (10 mM) at 275−288 mOsm. Cells were voltage clamped at −60 mV using an Axopatch 200A integrating patch clamp (Axon Instruments). Recordings were made using Axograph 10 and Chart 5.5. Dopamine neurons were identified by location, size, firing properties, and response to dopamine.

Dopamine Receptor Activation Experiments on Brain Slice. CyHQ-*O*-DA was kept as a stock solution in DMSO (50 mM) and diluted with modified Krebs buffer to a working concentration of 50−150 μM that recirculated through the tissue preparation. CyHQ-sulpiride was kept as a stock solution in DMSO (10 mM) and diluted to a 5 μM working solution. A ThorLabs M365LP1-C1 LED was used to photolyze CyHQ compounds at 0.5−1.8 mW of 365 nm light for 1−300 ms and 7 mW for 50−1000 ms for CyHQ-*O*-DA and CyHQ-sulpiride, respectively. Dopamine IPSCs were elicited by a single stimulation (0.5 ms) from an A360 WPI Stimulus Isolator and a fork electrode placed medially in comparison to the cell being patched. Dopamine iontophoresis was done using a thin-walled glass electrode (70−110 MΩ) with its tip placed within 10 μm of the soma that was filled with 1 M dopamine, which was kept in place with a 4 nA backing current and ejected with a 10 ms, 100 nA pulse. Iontophoresis was controlled by an Axoclamp-2a amplifier. Dopamine and baclofen for superperfusion were dissolved in water and kept at 4 °C. Statistical analysis for these experiments were performed using Prism 7 statistical software to calculate one-way ANOVA with Tukey correction for multiple comparison or t tests where applicable.

■ ASSOCIATED CONTENT

Supporting Information

The Supporting Information is available free of charge at https://pubs.acs.org/doi/10.1021/acschemneuro.9b00675.

Scheme S1, Figures S1−S8, Tables S1 and S2, HPLC traces, and spectroscopic data (PDF)

https://dx.doi.org/10.1021/acschemneuro.9b00675
ACS Chem. Neurosci. 2020, 11, 939−951

AUTHOR INFORMATION

Corresponding Authors

Timothy M. Dore − *New York University Abu Dhabi, Abu Dhabi, United Arab Emirates; Department of Chemistry, University of Georgia, Athens, Georgia 30602, United States;* orcid.org/0000-0002-3876-5012; Email: timothy.dore@nyu.edu

John T. Williams − *Vollum Institute, Oregon Health and Science University, Portland, Oregon 97239, United States;* orcid.org/0000-0002-0647-6144; Email: williamj@ohsu.edu

Authors

Naeem Asad − *New York University Abu Dhabi, Abu Dhabi, United Arab Emirates;* orcid.org/0000-0001-6871-5270

Duncan E. McLain − *New York University Abu Dhabi, Abu Dhabi, United Arab Emirates; Department of Chemistry, University of Georgia, Athens, Georgia 30602, United States*

Alec F. Condon − *Vollum Institute, Oregon Health and Science University, Portland, Oregon 97239, United States;* orcid.org/0000-0003-2655-2121

Sangram Gore − *New York University Abu Dhabi, Abu Dhabi, United Arab Emirates;* orcid.org/0000-0003-4236-7604

Shahienaz E. Hampton − *New York University Abu Dhabi, Abu Dhabi, United Arab Emirates;* orcid.org/0000-0002-6600-9492

Sauparnika Vijay − *New York University Abu Dhabi, Abu Dhabi, United Arab Emirates*

Complete contact information is available at: https://pubs.acs.org/10.1021/acschemneuro.9b00675

Funding

This research was supported by New York University Abu Dhabi and in part by grants to T.M.D. from the U.S. National Institutes of Health (R01 NS070159) and the U.S. National Science Foundation (CHE-1012412 and CHE-1317760), to J.T.W. from the U.S. National Institutes of Health (R01 DA004523), and to A.F.C. from the U.S. National Institutes of Health (F31 DA047007).

Notes

The authors declare no competing financial interest.

ACKNOWLEDGMENTS

Part of this work was carried out using Core Technology Platform resources at New York University Abu Dhabi. We thank Davide Deodato, Brooks G. Robinson, David Weiner, and Samuel S.−H. Wang for helpful discussions.

REFERENCES

(1) Neve, K. A. (2004) Dopamine receptors. In *Encycl. Biol. Chem.*; Lennarz, W. J., and Lane, M. D., Eds.; Vol. *1*, p 817−822.

(2) Beaulieu, J.-M., and Gainetdinov, R. R. (2011) The physiology, signaling, and pharmacology of dopamine receptors. *Pharmacol. Rev. 63*, 182−217.

(3) Surmeier, D. J., Graves, S. M., and Shen, W. (2014) Dopaminergic modulation of striatal networks in health and Parkinson's disease. *Curr. Opin. Neurobiol. 29*, 109−117.

(4) Martorana, A., and Koch, G. (2014) Is dopamine involved in Alzheimer's disease? *Front. Aging Neurosci. 6*, 252/1−252/17.

(5) Chuhma, N., Mingote, S., Kalmbach, A., Yetnikoff, L., and Rayport, S. (2017) Heterogeneity in Dopamine Neuron Synaptic Actions Across the Striatum and Its Relevance for Schizophrenia. *Biol. Psychiatry 81*, 43−51.

(6) Nestler, E. J., and Luscher, C. (2019) The molecular basis of drug addiction: linking epigenetic to synaptic and circuit mechanisms. *Neuron 102*, 48−59.

(7) Cousins, D. A., Butts, K., and Young, A. H. (2009) The role of dopamine in bipolar disorder. *Bipolar Disord. 11*, 787−806.

(8) Arnsten Amy, F. T. (2006) Fundamentals of attention-deficit/hyperactivity disorder: circuits and pathways. *J. Clin. Psychiatry 67*, 7−12.

(9) Bromberg-Martin, E. S., Matsumoto, M., and Hikosaka, O. (2010) Dopamine in Motivational Control: Rewarding, Aversive, and Alerting. *Neuron 68*, 815−834.

(10) Iordanova, M. D. (2019) Dopamine Signaling Is Critical for Supporting Cue-Driven Behavioral Control. *Neuroscience 412*, 257−258.

(11) Tritsch, N. X., and Sabatini, B. L. (2012) Dopaminergic Modulation of Synaptic Transmission in Cortex and Striatum. *Neuron 76*, 33−50.

(12) Ford, C. P., Phillips, P. E. M., and Williams, J. T. (2009) The time course of dopamine transmission in the ventral tegmental area. *J. Neurosci. 29*, 13344−13352.

(13) Gantz, S. C., Bunzow, J. R., and Williams, J. T. (2013) Spontaneous Inhibitory Synaptic Currents Mediated by a G Protein-Coupled Receptor. *Neuron 78*, 807−812.

(14) Courtney, N. A., and Ford, C. P. (2014) The timing of dopamine- and noradrenaline-mediated transmission reflects underlying differences in the extent of spillover and pooling. *J. Neurosci. 34*, 7645−7656.

(15) Vandenbergh, D. J. (2008) Cloning and genetic analysis of dopamine transporters. *Dopamine Transp.*, 47−71.

(16) Vaughan, R. A., and Foster, J. D. (2013) Mechanisms of dopamine transporter regulation in normal and disease states. *Trends Pharmacol. Sci. 34*, 489−496.

(17) Lohr, K. M., Masoud, S. T., Salahpour, A., and Miller, G. W. (2017) Membrane transporters as mediators of synaptic dopamine dynamics: implications for disease. *Eur. J. Neurosci. 45*, 20−33.

(18) Salatino-Oliveira, A., Rohde, L. A., and Hutz, M. H. (2018) The dopamine transporter role in psychiatric phenotypes. *Am. J. Med. Genet., Part B 177*, 211−231.

(19) Kramer, R. H., and Chambers, J. J., Eds. (2011) *Photosensitive Molecules for Controlling Biological Function*, Humana Press, New York.

(20) Klán, P., Šolomek, T., Bochet, C. G., Blanc, A., Givens, R., Rubina, M., Popik, V., Kostikov, A., and Wirz, J. (2013) Photoremovable Protecting Groups in Chemistry and Biology: Reaction Mechanisms and Efficacy. *Chem. Rev. 113*, 119−191.

(21) Hall, H., Sallemark, M., and Jerning, E. (1986) Effects of remoxipride and some related new substituted salicylamides on rat brain receptors. *Acta Pharmacol. Toxicol. 58*, 61−70.

(22) Koehler, C., Hall, H., Magnusson, O., Lewander, T., and Gustafsson, K. (1990) Biochemical pharmacology of the atypical neuroleptic remoxipride. *Acta Psychiatr. Scand. 82*, 27−36.

(23) Furman, C. A., Roof, R. A., Moritz, A. E., Miller, B. N., Doyle, T. B., Free, R. B., Banala, A. K., Paul, N. M., Kumar, V., Sibley, C. D., Newman, A. H., and Sibley, D. R. (2015) Investigation of the binding and functional properties of extended length D3 dopamine receptor-selective antagonists. *Eur. Neuropsychopharmacol. 25*, 1448−1461.

(24) Lee, T. H., Gee, K. R., Ellinwood, E. H., and Seidler, F. J. (1996) Combining "caged-dopamine" photolysis with fast-scan cyclic voltammetry to assess dopamine clearance and release autoinhibition in vitro. *J. Neurosci. Methods 67*, 221−231.

(25) Araya, R., Andino-Pavlovsky, V., Yuste, R., and Etchenique, R. (2013) Two-Photon Optical Interrogation of Individual Dendritic Spines with Caged Dopamine. *ACS Chem. Neurosci. 4*, 1163−1167.

(26) Hagen, V., Kilic, F., Schaal, J., Dekowski, B., Schmidt, R., and Kotzur, N. (2010) [8-[Bis(carboxymethyl)aminomethyl]-6-bromo-7-hydroxycoumarin-4-yl]methyl Moieties as Photoremovable Protecting Groups for Compounds with COOH, NH2, OH, and C:O Functions. *J. Org. Chem. 75*, 2790−2797.

(27) Robinson, B. G., Bunzow, J. R., Williams, J. T., Grimm, J. B., Lavis, L. D., Dudman, J. T., Brown, J., and Neve, K. A. (2017)

Desensitized D2 autoreceptors are resistant to trafficking. *Sci. Rep. 7*, 4379.
(28) Milburn, T., Matsubara, N., Billington, A. P., Udgaonkar, J. B., Walker, J. W., Carpenter, B. K., Webb, W. W., Marque, J., and Denk, W. (1989) Synthesis, photochemistry, and biological activity of a caged photolabile acetylcholine receptor ligand. *Biochemistry 28*, 49−55.
(29) Breitinger, H.-G. A., Wieboldt, R., Ramesh, D., Carpenter, B. K., and Hess, G. P. (2000) Synthesis and Characterization of Photolabile Derivatives of Serotonin for Chemical Kinetic Investigations of the Serotonin 5-HT3 Receptor. *Biochemistry 39*, 5500−5508.
(30) Russell, A. G., Sadler, M. J., Laidlaw, H. J., Gutierrez-Loriente, A., Wharton, C. W., Carteau, D., Bassani, D. M., and Snaith, J. S. (2012) Photorelease of tyrosine from α-carboxy-6-nitroveratryl (αCNV) derivatives. *Photochem. Photobiol. Sci. 11*, 556−563.
(31) Kiskin, N. I., and Ogden, D. (2002) Two-photon excitation and photolysis by pulsed laser illumination modelled by spatially non-uniform reactions with simultaneous diffusion. *Eur. Biophys. J. 30*, 571−587.
(32) Kiskin, N. I., Chillingworth, R., McCray, J. A., Piston, D., and Ogden, D. (2002) The efficiency of two-photon photolysis of a ″caged″ fluorophore, *o*-1-(2-nitrophenyl)ethylpyranine, in relation to photodamage of synaptic terminals. *Eur. Biophys. J. 30*, 588−604.
(33) Il'ichev, Y. V., Schwoerer, M. A., and Wirz, J. (2004) Photochemical Reaction Mechanisms of 2-Nitrobenzyl Compounds: Methyl Ethers and Caged ATP. *J. Am. Chem. Soc. 126*, 4581−4595.
(34) Corrie, J. E. T., Munasinghe, V. R. N., Trentham, D. R., and Barth, A. (2008) Studies of decarboxylation in photolysis of α-carboxy-2-nitrobenzyl (CNB) caged compounds. *Photochem. Photobiol. Sci. 7*, 84−97.
(35) Corrie, J. E. T., Barth, A., Munasinghe, V. R. N., Trentham, D. R., and Hutter, M. C. (2003) Photolytic Cleavage of 1-(2-Nitrophenyl)ethyl Ethers Involves Two Parallel Pathways and Product Release Is Rate-Limited by Decomposition of a Common Hemiacetal Intermediate. *J. Am. Chem. Soc. 125*, 8546−8554.
(36) Papageorgiou, G., and Corrie, J. E. T. (1997) Synthesis and properties of carbamoyl derivatives of photolabile benzoins. *Tetrahedron 53*, 3917−3932.
(37) Papageorgiou, G., Barth, A., and Corrie, J. E. T. (2005) Flash photolytic release of alcohols from photolabile carbamates or carbonates is rate-limited by decarboxylation of the photoproduct. *Photochem. Photobiol. Sci. 4*, 216−220.
(38) Gilbert, D., Funk, K., Dekowski, B., Lechler, R., Keller, S., Moehrlen, F., Frings, S., and Hagen, V. (2007) Caged capsaicins: new tools for the examination of TRPV1 channels in somatosensory neurons. *ChemBioChem 8*, 89−97.
(39) Warther, D., Gug, S., Specht, A., Bolze, F., Nicoud, J. F., Mourot, A., and Goeldner, M. (2010) Two-photon uncaging: New prospects in neuroscience and cellular biology. *Bioorg. Med. Chem. 18*, 7753−7758.
(40) Dore, T. M., and Wilson, H. C. (2011) Chromophores for the Delivery of Bioactive Molecules with Two-Photon Excitation. In *Photosensitive Molecules for Controlling Biological Function*; Chambers, J. J., and Kramer, R. H., Eds.; pp 57−92, Humana Press, New York.
(41) Bort, G., Gallavardin, T., Ogden, D., and Dalko, P. I. (2013) From One-Photon to Two-Photon Probes: ″Caged″ Compounds, Actuators, and Photoswitches. *Angew. Chem., Int. Ed. 52*, 4526−4537.
(42) Abe, M., Chitose, Y., Jakkampudi, S., Thuy, P. T. T., Lin, Q., Van, B. T., Yamada, A., Oyama, R., Sasaki, M., and Katan, C. (2017) Design and Synthesis of Two-Photon Responsive Chromophores for Near-Infrared Light-Induced Uncaging Reactions. *Synthesis 49*, 3337−3346.
(43) Aujard, I., Benbrahim, C., Gouget, M., Ruel, O., Baudin, J.-B., Neveu, P., and Jullien, L. (2006) *o*-Nitrobenzyl photolabile protecting groups with red-shifted absorption: syntheses and uncaging cross-sections for one- and two-photon excitation. *Chem. - Eur. J. 12*, 6865−6879.
(44) Gienger, M., Hübner, H., Löber, S., König, B., and Gmeiner, P. (2020) Structure-based development of caged dopamine D2/D3 receptor antagonists. *Sci. Rep. 10*, 829.
(45) Davis, M. J., Kragor, C. H., Reddie, K. G., Wilson, H. C., Zhu, Y., and Dore, T. M. (2009) Substituent Effects on the Sensitivity of a Quinoline Photoremovable Protecting Group to One- and Two-Photon Excitation. *J. Org. Chem. 74*, 1721−1729.
(46) McLain, D. E., Rea, A. C., Widegren, M. B., and Dore, T. M. (2015) Photoactivatable, biologically-relevant phenols with sensitivity toward 2-photon excitation. *Photochem. Photobiol. Sci. 14*, 2151−2158.
(47) Asad, N., Deodato, D., Lan, X., Widegren, M. B., Phillips, D. L., Du, L., and Dore, T. M. (2017) Photochemical Activation of Tertiary Amines for Applications in Studying Cell Physiology. *J. Am. Chem. Soc. 139*, 12591−12600.
(48) O'Connor, M. J., Beebe, L. L., Deodato, D., Ball, R. E., Page, A. T., VanLeuven, A. J., Harris, K. T., Park, S., Hariharan, V., Lauderdale, J. D., and Dore, T. M. (2019) Bypassing Glutamic Acid Decarboxylase 1 (Gad1) Induced Craniofacial Defects with a Photoactivatable Translation Blocker Morpholino. *ACS Chem. Neurosci. 10*, 266−278.
(49) Pettit, D. L., Wang, S. S. H., Gee, K. R., and Augustine, G. J. (1997) Chemical two-photon uncaging: a novel approach to mapping glutamate receptors. *Neuron 19*, 465−471.
(50) Khalil, I. M., Barker, D., and Copp, B. R. (2016) Bioinspired Syntheses of the Pyridoacridine Marine Alkaloids Demethyldeoxyamphimedine, Deoxyamphimedine, and Amphimedine. *J. Org. Chem. 81*, 282−289.
(51) Ma, J., Rea, A. C., An, H., Ma, C., Guan, X., Li, M.-D., Su, T., Yeung, C. S., Harris, K. T., Zhu, Y., Nganga, J. L., Fedoryak, O. D., Dore, T. M., and Phillips, D. L. (2012) Unraveling the Mechanism of the Photodeprotection Reaction of 8-Bromo- and 8-Chloro-7-hydroxyquinoline Caged Acetates. *Chem. - Eur. J. 18*, 6854−6865.
(52) Ma, J., Mewes, J.-M., Harris, K. T., Dore, T. M., Phillips, D. L., and Dreuw, A. (2017) Unravelling the early photochemical behavior of (8-substituted-7-hydroxyquinolinyl)methyl acetates through electronic structure theory and ultrafast transient absorption spectroscopy. *Phys. Chem. Chem. Phys. 19*, 1089−1096.
(53) Huang, J., Muliawan, A. P., Ma, J., Li, M. D., Chiu, H. K., Lan, X., Deodato, D., Phillips, D. L., and Dore, T. M. (2017) A spectroscopic study of the excited state proton transfer processes of (8-bromo- 7-hydroxyquinolin-2-yl)methyl-protected phenol in aqueous solutions. *Photochem. Photobiol. Sci. 16*, 575−584.
(54) Salierno, M., Marceca, E., Peterka, D. S., Yuste, R., and Etchenique, R. (2010) A fast ruthenium polypyridine cage complex photoreleases glutamate with visible or IR light in one and two photon regimes. *J. Inorg. Biochem. 104*, 418−422.
(55) Panjehpour, M., Castro, M., and Klotz, K.-N. (2005) Human breast cancer cell line MDA-MB-231 expresses endogenous A2B adenosine receptors mediating a Ca2+ signal. *Br. J. Pharmacol. 145*, 211−218.
(56) Borcherding, D. C., Tong, W., Hugo, E. R., Barnard, D. F., Fox, S., LaSance, K., Shaughnessy, E., and Ben-Jonathan, N. (2016) Expression and therapeutic targeting of dopamine receptor-1 (D1R) in breast cancer. *Oncogene 35*, 3103−3113.
(57) Lacey, M. G., Mercuri, N. B., and North, R. A. (1990) Actions of cocaine on rat dopaminergic neurons in vitro. *Br. J. Pharmacol. 99*, 731−735.
(58) de Witte, W. E. A., Versfelt, J. W., Kuzikov, M., Rolland, S., Georgi, V., Gribbon, P., Gul, S., Huntjens, D., van der Graaf, P. H., Danhof, M., Fernandez-Montalvan, A., Witt, G., and de Lange, E. C. M. (2018) In vitro and in silico analysis of the effects of D2 receptor antagonist target binding kinetics on the cellular response to fluctuating dopamine concentrations. *Br. J. Pharmacol. 175*, 4121−4136.
(59) Lepiku, M., Rinken, A., Jarv, J., and Fuxe, K. (1997) Modulation of [3H]quinpirole binding to dopaminergic receptors by adenosine A2A receptors. *Neurosci. Lett. 239*, 61−64.
(60) Furuta, T., Wang, S. S. H., Dantzker, J. L., Dore, T. M., Bybee, W. J., Callaway, E. M., Denk, W., and Tsien, R. Y. (1999) Brominated 7-hydroxycoumarin-4-ylmethyls: photolabile protecting groups with

https://dx.doi.org/10.1021/acschemneuro.9b00675
ACS Chem. Neurosci. 2020, 11, 939−951

biologically useful cross-sections for two photon photolysis. *Proc. Natl. Acad. Sci. U. S. A. 96*, 1193−1200.
(61) Hennig, A.-L. K., Deodato, D., Asad, N., Herbivo, C., and Dore, T. M. (2020) Two-Photon Excitable Photoremovable Protecting Groups Based on the Quinoline Scaffold for Use in Biology. *J. Org. Chem. 85*, 726−744.

https://dx.doi.org/10.1021/acschemneuro.9b00675
ACS Chem. Neurosci. 2020, 11, 939−951